

# **RESULTS OF THE PRE-NORMATIVE RESEARCH PROJECT PRESLHY FOR THE SAFE USE OF LIQUID HYDROGEN**

**Jordan, T.<sup>1</sup>, Bernard, L.<sup>2</sup>, Cirrone, D.<sup>7</sup>, Coldrick, S.<sup>3</sup>, Friedrich, A.<sup>6</sup>, Jallais, S.<sup>2</sup>, Kuznetsov, M.<sup>1</sup>,  
Proust, C.<sup>4</sup>, Venetsanos, A.<sup>5</sup>, and Wen, J.<sup>8</sup>**

**<sup>1</sup> Karlsruhe Institute of Technology, PO Box 3640, Karlsruhe, 76646, Germany, jordan@kit.edu**

**<sup>2</sup> Air Liquide, Paris Innovation Campus, France**

**<sup>3</sup>Health & Safety Executive, Buxton, UK**

**<sup>4</sup>INERIS, Verneuil-en-Halatte, France**

**<sup>5</sup>National Center for Scientific Research Demokritos, Athens, Greece**

**<sup>6</sup>Pro-Science, Ettlingen, Germany**

**<sup>7</sup>University of Ulster, Belfast, UK**

**<sup>8</sup>University of Warwick, Coventry, UK**

## **ABSTRACT**

Liquid hydrogen (LH2) compared to compressed gaseous hydrogen offers advantages for large-scale transport and storage of hydrogen with higher densities. Although the gas industry has good experience with LH2 only little experience is available for the new applications of LH2 as an energy carrier. Therefore, the European FCH JU funded project PRESLHY conducted pre-normative research for the safe use of cryogenic LH2 in non-industrial settings. The central research consisted of a broad experimental program, combined with analytical work, modelling and simulations belonging to the three key phenomena of the accident chain: release and mixing, ignition and combustion. The presented results improve the general understanding of the behavior of LH2 in accidents and provide some design guidelines and engineering tools for safer use of LH2. Recommendations for improvement of current international standards are derived.

## **1.0 MOTIVATION AND OBJECTIVES**

For scaling up the hydrogen supply infrastructure the transport of liquefied hydrogen is the most effective option due to the energy density and implicit purity. Especially for the transport sector with the planned large bus fleets, the emerging hydrogen fuelled trains, ships and heavy duty trucks projects and even for the pre-cooled 70 MPa light duty vehicles refuelling liquid hydrogen (LH2) or cryogenic hydrogen in general offer sufficient densities and efficiency gains over gaseous transport, storage and supply. However, cryogenic hydrogen implies specific hazards and risks, which are very different from those associated with the relatively well-known compressed gaseous hydrogen. Although these specific issues are usually well reflected and managed in large-scale industry and aerospace applications, experience with cryogenic hydrogen in a distributed energy system is lacking. Transport and storage of LH2 in urban areas and the daily use by the untrained general public will require higher levels of safety provisions accounting for the very special properties. The quite different operational conditions compared with the industrial environment and therefore also different potential accident scenarios will put an emphasis on specific, related phenomena which are not well understood. Specific recommendations and harmonised performance-based international standards are lacking for similar reasons.

Therefore, the European pre-normative research project PRESLHY - Pre-normative REsearch for Safe Use of Liquid HYdrogen - assessed relevant and poorly understood phenomena related to high risk scenarios. With the new knowledge generated by the project science-based and validated tools, which

are required for hydrogen safety engineering and risk-informed, performance-based, LH2 specific, international standards, have been developed.

The main results of PRESLHY are

- new validation data generated by an experimental program addressing release, ignition and combustion phenomena,
- a collection of models and engineering correlations suitable for integration in any risk assessment toolkit,
- an update of the state-of-the-art captured in the special report “Handbook of hydrogen safety: Chapter on LH2 safety”,
- recommendations for safe design and operations of LH2 technologies and
- recommendations for updating of existing international standards and development of new specific performance-based and risk-informed standards.

The more detailed results are contained in 47 deliverables, 29 of them published on the project website [www.preslhy.eu](http://www.preslhy.eu).

## 2.0 GENERAL ASPECTS OF THE PROJECT

The PRESLHY project started in January 2018 and was initially funded for a three-year duration. With an extension of 5 months the funded period ended in May 2021. The project consortium consisted of 9 partners from 5 European countries: Karlsruhe Institute of Technology (KIT, coordinator), Air Liquide (AL), INERIS, Health & Safety Laboratory (HSL), HySafe, National Center for Scientific Research Demokritos (NCSR), Pro-Science (PS) University of Ulster (UU) and University of Warwick (UWAR).

As shown in Figure 1 the work was structured into the work packages WP2 for Technical Strategy & Evaluation, the phenomenological WP3 Release & Mixing, WP4 Ignition, WP5 Combustion and WP6 for Implementation and Dissemination. Management and administration was organised in WP1.

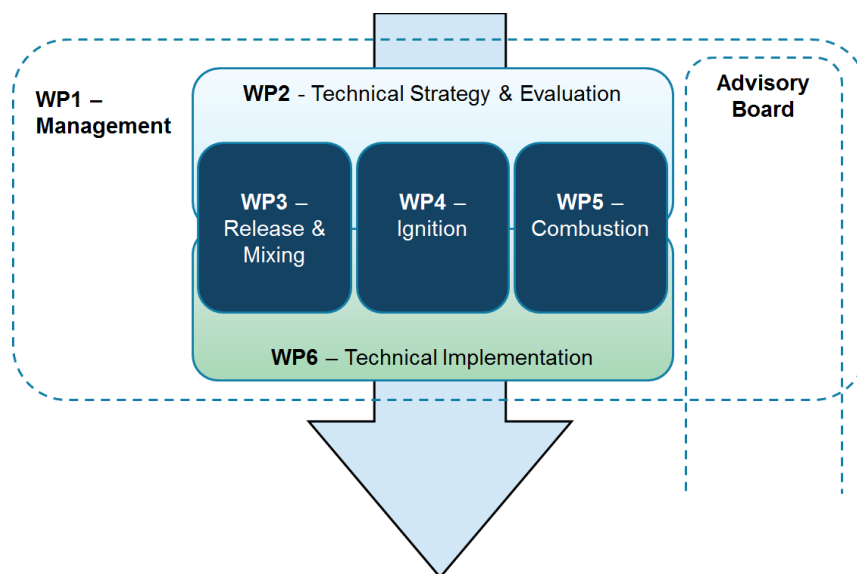


Figure 1: General approach of the PRESLHY project.

The advisory board was organised by HySafe and was composed of international experts from industry and from standards developing organisations (SDO), extending the reach of the project's impact internationally to mainly US and Japan. The networking has been further expanded by reaching out to the US DoE program H2@scale via HySafe members SNL and PNNL and to the Norwegian project SH2IFT via HySafe members GexCon, DNV and Equinor.

The following chapters will present the results achieved in WP2 to WP6.

### **3.0 RESULTS OF WP2 - TECHNICAL STRATEGY AND STATE-OF-THE-ART**

WP2 set the stage for by summarising the state-of-the-art, identifying critical knowledge gaps and key scenarios and providing a refined work program at the initial phase of the project. An analysis of existing Regulations, Code and Standards (RCS) as well as industry best practices was conducted. The corresponding report [16] emphasises the importance of determining science based hazard distances for liquid hydrogen installations and then compare them with the requirements of the published RCS. Secondly, a description of prototypical LH2 installations was provided [11]. Thirdly, a bibliographic State of the Art (SoA) study was performed [10]. This report focusses on experimental and modelling work on release/mixing phenomena, ignition phenomena and combustion phenomena. The objective of the SoA was to identify the remaining knowledge gaps.

A Phenomena Identification and Ranking Table (PIRT) was also performed in September 2018. PIRT is a systematic way of gathering information from experts on a specific subject, here LH2 safety, and ranking the importance of the information, in order to meet some decision-making objectives, e.g., determining what are the highest priorities for research and development on that subject. A PIRT questionnaire was prepared and widely distributed thanks to the large network of all PRESLHY members, in particular HySafe. For the work packages WP3-5 a list of associated physical phenomena was developed. For each phenomenon identified, the participants ranked the general level of understanding, level of maturity of engineering modelling, level of maturity of CFD modelling, availability of experimental data, and criticality for enabling LH2 in populated areas. The final knowledge scores and ranking results are provided in [12].

The SoA and the PIRT concluded on the need for additional research on the physics of the liquid releases (internal flashing, droplets, rainout, condensation, external flashing, ...), on the electrostatic ignition and LH2 / solid oxygen ignition and on the deflagration, detonation and flame acceleration in cold conditions. Based on these conclusions, the experimental work program was updated.

### **4.0 RESULTS OF WP3 - PHENOMENA RELEASE AND MIXING**

#### **4.1 Modelling and simulation of release and mixing**

On the modelling and simulation side a CFD inter-comparison exercise on steady cryogenic gaseous hydrogen jets was organized based on the experiments by SNL [9]. For the inter-comparison two tests were selected with 1 mm nozzle and stagnation conditions 0.2 MPa, 58 K and 0.5 MPa, 50 K and two tests with 1.25 mm nozzle, with stagnation conditions 0.2 MPa, 61 K and 0.4 MPa, 54 K. Four partners AL, KIT, NCSRD and UU participated in the exercise with different CFD codes (FLACS, GASFLOW-MPI, ADREA-HF and FLUENT respectively) and modelling strategies (LES for KIT and RANS for the others). Figure 2 shows predicted concentration and temperature distribution along the jet centreline compared to experimental data for stagnation conditions 0.5 MPa, 50 K and nozzle diameter 1mm. The influence of the chosen virtual nozzle concept is discussed. The influence of the real gas behaviour is negligible.

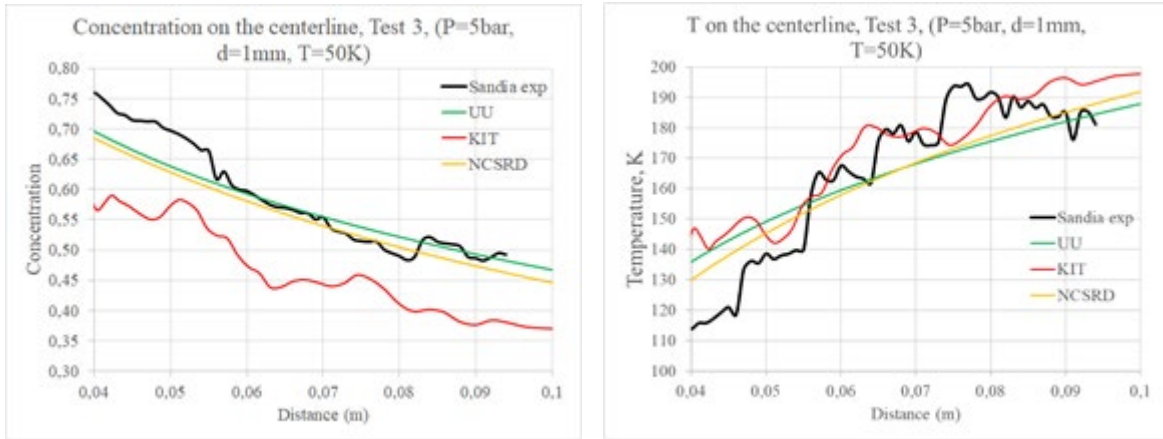


Figure 2: Predicted and measured concentration (right frame) temperature (left frame) at the along the jet centreline (1mm, 0.2 MPa, 50 K).

UWAR carried out corresponding numerical simulations of under-expanded hydrogen jets. They considered both the near-field flow physics and the far-field hydrogen dispersion. For the near-field regime, the detailed flow structures and the transient physics of the under-expanded cryogenic hydrogen jets are numerically analysed with high-resolution direct numerical simulations (DNS). The early stages of the near-nozzle flow structures from time  $t = 10$  to  $40 \mu\text{s}$  are shown in Figure 3(a). Complex waves are formed in the near-nozzle field. If the partial pressure of hydrogen ( $P_{H_2}$ ) is higher than its saturated vapour pressure ( $P_{vap}$ ), the localized hydrogen liquefaction is expected to occur (domain within red dashed lines in Figure 3(a)). The downstream development of the jets is shown in Figure 3(b). The regime of the potential liquefaction region decreases continuously as the expansion wave weakens. The variation in the nozzle pressure ratio did not only affect the hydrogen dispersion but also the jet shapes. The jet head varies from a round shape for the low nozzle pressure ratio to a quasi-rectangle shape for the high nozzle pressure ratio.

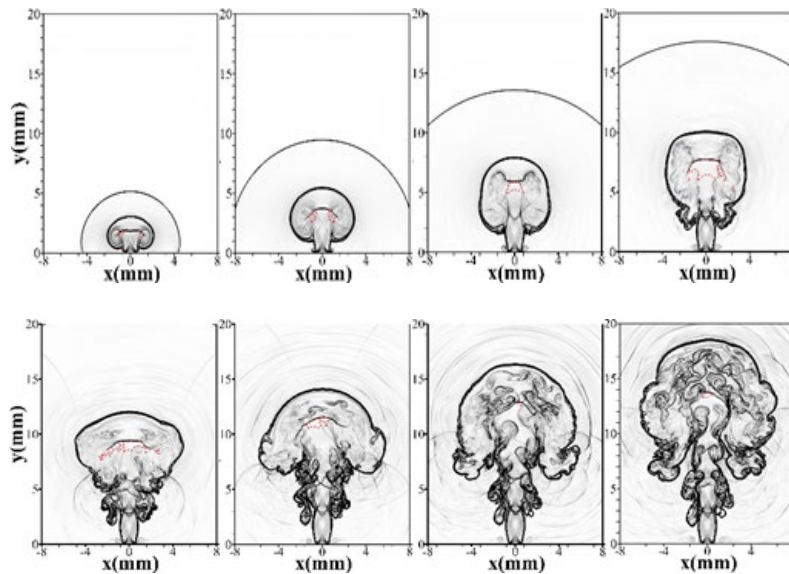


Figure 3: Instantaneous distributions of density gradient: (a) from time = 10 to  $40 \mu\text{s}$  and (b) from time = 50 to  $80 \mu\text{s}$ . The red dashed lines denote the region of  $HLP > 0$ .

For the far-field dispersion of hydrogen, the large eddy simulation (LES) of the of the blowdown process has been conducted by using rhoReactingFOAM within the frame of open-source CFD code OpenFOAM. For comparison, the Reynolds-averaged Navier-Stokes (RANS) approach has also been used with the RNG k-epsilon turbulence model for turbulence. It is found that the LES approach predicts a more rapid dispersion of hydrogen than that of RANS.

However, it has been shown that concentration decay in momentum-dominated hydrogen jets at cryogenic temperatures obey the same similarity law currently widely used for ambient temperature in hydrogen safety engineering.

In the framework of developing simplified engineering models NCSR developed an engineering tool for cryogenic and ambient release calculations. The tool takes into account discharge line effects (friction, area change, extra resistance due to fittings and heat transfer through pipe walls). Stagnation conditions are either assumed adiabatic or provided as input. Single phase physical properties are calculated using the HFE formulation. Phase distribution is calculated with HEM or various HNEM models. The tool was validated against a series of steady and transient release experiments either pre-existing or performed within PRESLHY, see [18][19][20][21][22]. Ulster University performed analytical and computational modelling to assess the effect of heat transfer through the wall of a storage tank and discharge pipe system, which are not properly insulated [6]. The analytical modelling of a storage tank blowdown showed that experimental temperature dynamics in a tank could be reproduced accurately if heat transfer effect through a tank wall and discharge pipe was included, conversely to the case approaching the adiabatic limit. Measurements from DISCHA tests performed within PRESLHY by partner Pro-Science were used for comparison with calculations. Numerical simulations by Ulster University on cryogenic hydrogen flow in a release pipe exposed to ambient air showed that the experimental mass flow rate could be reproduced only by taking into account heat transfer through the wall of the release system. The effect was seen to increase with the storage pressure.

A parametric CFD analysis of the BLEVE phenomenon was conducted by means of the CFD code ADREA-HF for LH2 vessels [17]. This work was performed in the context of PRESLHY and SH2IFT projects' collaboration. Firstly, the CFD model was validated against the well-documented CO<sub>2</sub> BLEVE experiment. Next, hydrogen BLEVE cases are examined. The physical parameters were chosen based on the BMW tests carried out in the 1990s on LH2 tanks designed for automotive purposes. Different filling degrees, initial pressures and temperatures of the tank content were simulated to comprehend how the blast wave is influenced by the initial conditions. Good agreement was shown between the simulation outcomes and the experimental results.

#### **4.1 Release and mixing experiments**

Experimental work within this work package includes the DISCHA and CRYOSTAT release experiments and the pool experiments by PS/KIT and the rainout experiments by HSE, all performed with cryogenic hydrogen.

PS/KIT DISCHA and CRYOSTAT experimental facilities are presented in Figure 4 below. In total more than 200 experiments with four circular nozzle diameters ( $d_N = 0.5, 1, 2, 4$  mm) and seven initial pressure stages ( $p_{ini} = 0.5, 1, 2, 5, 10, 15, 20$  MPa) were performed with the DISCHA-facility. 126 were conducted at ambient temperature and 88 at a temperature of approximately 80 K. For the cold tests the DISCHA-vessel ( $V = 2.85$  dm<sup>3</sup>) and the valve were cooled from outside by LN<sub>2</sub>. With the CRYOSTAT-facility ( $V = 225$  dm<sup>3</sup>) a second series of in total 12 release tests were performed. In 5 reference tests H<sub>2</sub> at ambient temperature was used. In 7 tests the CRYOSTAT-facility was filled with LH<sub>2</sub> at about 20 K. Two nozzles ( $d_N = 2$  and 4 mm) and an initial pressures up to 0.5 MPa were applied.



Figure 4: Photographs of the DISCHA-facility without (left) and with cooling box and additional equipment (center) as well as the CRYOSTAT-facility (right).

The release rates were calculated using accurate pressure and temperature measurements inside the vessel. Same quantities were also measured inside the release line, while downstream the nozzle temperature and H<sub>2</sub>-concentration measurements were performed to monitor the hydrogen dispersion after release. In most of the experiments two electric field mills were used to measure the electrostatic field generated during the release (results see below).

All external mixing processes of the releases have been video recorded and documented by photo-series that were post-processed with Background Oriented Schlieren (BOS)-algorithms, for example see Figure 5.

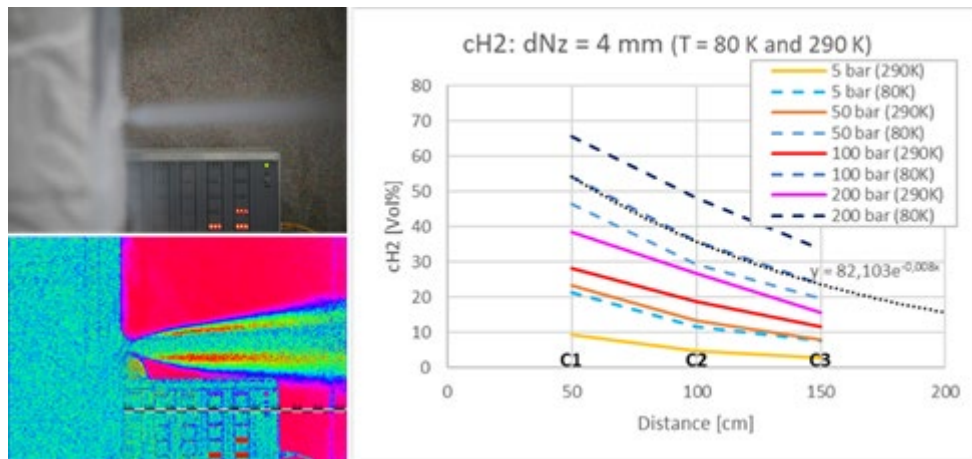


Figure 5: DISCHA-experiments: Original and BOS-processed images of nozzle (left) and examples for maximum measured H<sub>2</sub>-concentrations (right).

The measured pressure and temperature courses in the vessel allow determining release rates and the ex-vessel measurements enabled estimating the dispersion behaviour of the released hydrogen, also with respect to defining appropriate ignition locations for the variation of experiments, in which the H<sub>2</sub>-jets were ignited (see below). As an example the maximum measured H<sub>2</sub>-concentrations along the jet axis for release through the 4-mm nozzle together with one example for their extrapolation to larger distances is shown in the right graph of Figure 5.

A CFD inter-comparison exercise on the transient cryogenic gaseous hydrogen jets was also performed, see [7]. The selected DISCHA release test (20 MPa, 77 K, 4 mm nozzle) provided strongest effects and best quality in the measurements. Three partners participated in this exercise: NCSR, UU and UWAR, with different CFD codes (ADREA-HF, FLUENT and OpenFOAM) and modelling strategies (RANS and LES for UWAR). The predicted temperature time series were found in fairly good agreement with

the experiments. On the other hand, none of the models reproduced the relatively large arrival times of measured concentrations, suggesting that measurements of concentration close to the source for transient under-expanded hydrogen jets is a big challenge and needs further research supported by simulations.

The experimental setup for the PS/KIT POOL experiments is shown in Figure 6 below. The facility comprises mainly of an insulated square stainless-steel box (50 cm x 50 cm, height: 20 cm) on a scale. Three identical boxes were made and filled up to half the height (10 cm) with different substrates (concrete, sand, water and gravel).

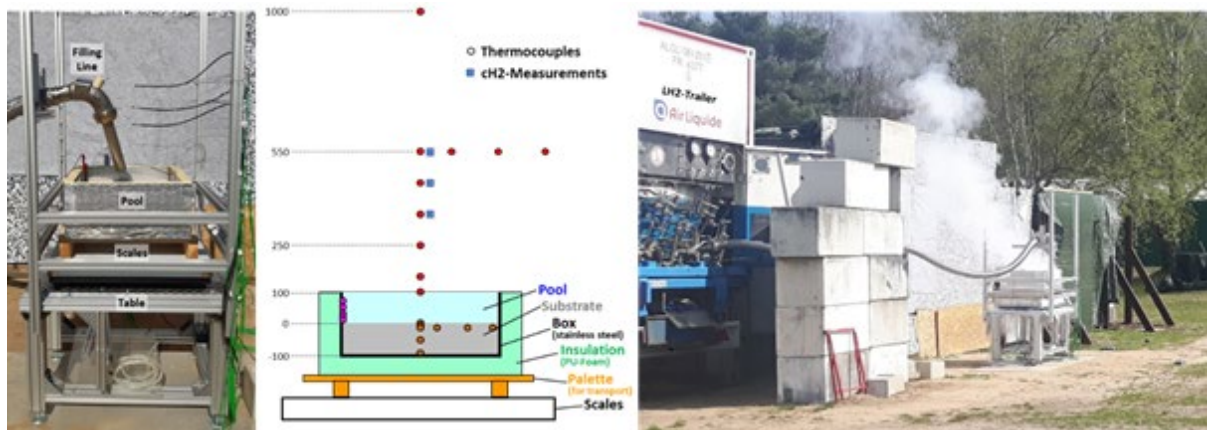


Figure 6: Photo and sketch of POOL-facility set-up (left) and snapshot of a POOL experiment (right).

Inside and above the substrate, as well as above the facility in total 24 thermocouples were distributed. Above the facility also three measurement positions for remote H<sub>2</sub>-concentration measurements were placed. Further instrumentation included optical observation and ambient wind measurements. In four of the ten experiments also a large fan was installed to investigate the influence of side wind on the formation and evaporation of LH<sub>2</sub> pools.

In most of the experiments the pool was filled three times with LH<sub>2</sub> until it started to overflow to investigate the influence of different initial temperatures of the substrate. After the fillings the pool was left to evaporate. The filling level of the pool was determined using the weight of the facility and the thermocouples inside the pool in different heights, which clearly indicated their coverage with LH<sub>2</sub> by a constant value of approx. 20 K, while they started to show higher transient values as soon as they were exposed to gaseous atmosphere. With this instrumentation the evaporation rates for the different substrates can be determined (Figure 7) and also the influence of side wind on this phenomenon. In all cases much faster evaporation rates were determined for side wind conditions ( $v_{\text{Wind}} \approx 5 \text{ m/s}$ ). A further important outcome of the experiments was information on the concentration distribution above the pools that was used to define the ignition position and point in time for a second experimental series in which the gas cloud above the pools is ignited.

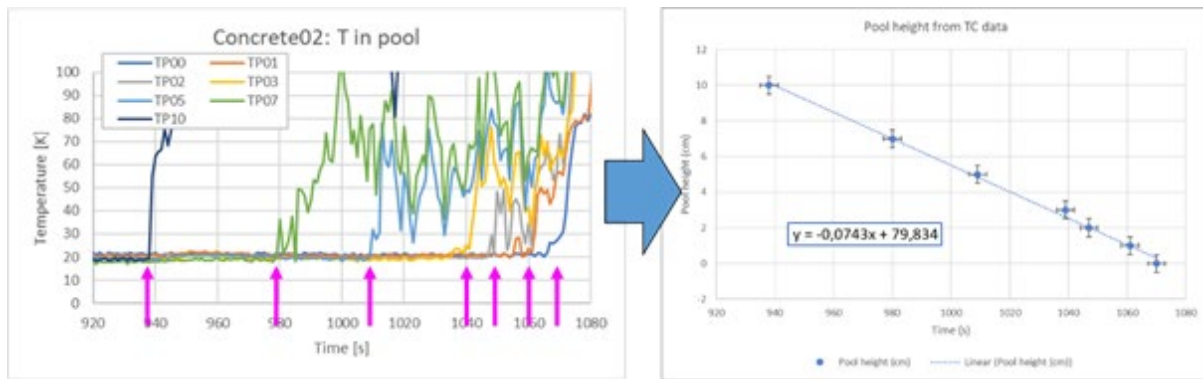


Figure 7: Example for determination of LH2-evaporation rate for experiment Concrete02.

HSE performed 18 large scale release experiments. From a LH2 trailer with a storage pressure of up to 0.5 MPa LH2 was release via an orifice (max 25,4 mm orifice diameter) with different release orientations. The release point was either 0.5 or 1.5 m above ground. The experiments were instrumented with pressure measurement in the trailer storage, mass flow meter of Coriolis type, measurements for determining electrical charge build-up and flow and the external domain was equipped with thermocouples, H2 and O2 concentration sensors. Additionally, an array of temperature and concentration sensors were installed in the mixing domain by a team of NREL in the frame of a bilateral agreement.

No rainout but strong ice formation on near field sensors was observed. The latter was disturbing the measurement process. However, the induced deflections of the sensors could be compensated. Only small electric fields associated with two-phase release effects have been observed and the induced electric current in the isolated pipe segment may be considered negligible. The temperature field measurements in the mixing zone should almost perfect correlation with concentration measurement.

For one of the large scale LH2 releases (test-11, 0.5 MPa tank pressure, 12mm nozzle, orifice  $d=25.4$  mm) another CFD inter-comparison study was conducted. Partners AL and NCSR D participated with FLACS and ADREA-HF codes respectively, see [8].

## 5.0 RESULTS OF WP4 - IGNITION PHENOMENA

The primary aim of WP4 was to understand scenarios that are unique to LH2, which may not have been previously addressed and which may introduce novel, previously unobserved and poorly understood pathways to ignition. These scenarios were studied through a combination of theoretical, numerical and experimental work. Initial theoretical studies were undertaken to establish how relevant ignition parameters, such as minimum ignition energy (MIE), relate to practical ignition sources such as electrical devices, electrostatics or hot surfaces. Based on the theoretical studies and identified gaps in understanding of related physical phenomena and their control, the experimental work covered the following areas:

### 5.1 Fundamental ignition parameters

A series of experiments was undertaken by INERIS to determine the influence of cryogenic temperatures on the evolution of standard ignition parameters as a function of temperature. The experimental programme was split into two parts; hot surface ignition of a flowing LH2-air mixture and minimum ignition energy (MIE) of an LH2-air mixture by spark generator (Figure 8). Ignition temperature by hot surface was found to be independent of mixture temperature, while stoichiometry

and flow velocity had a marginal influence. Measurements of MIE by spark ignition successfully reproduced reference tests at ambient temperature. Tests for hydrogen-air mixtures at  $-100^{\circ}\text{C}$  showed a slight increase in MIE.

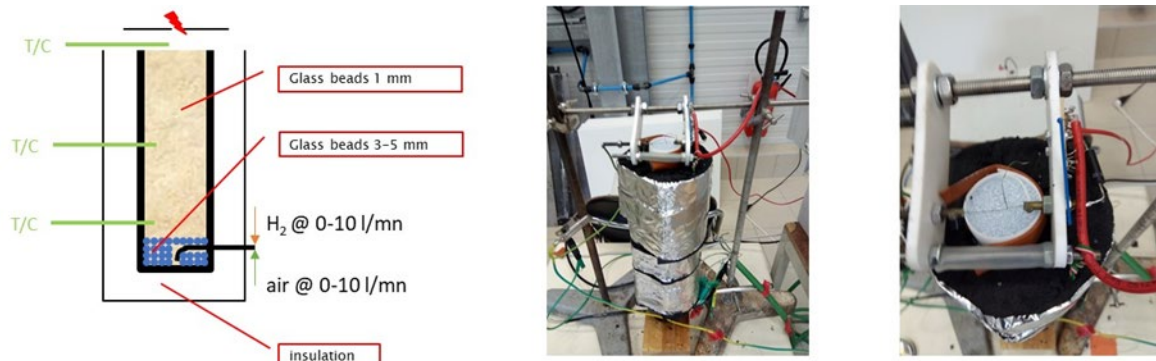


Figure 8: "Burner" device for measuring MIE using LH<sub>2</sub>-air flow through a pre-cooled bed.

To complement the theoretical and experimental aspects, University of Ulster developed numerical modelling techniques for the evaluation of MIE on spark ignition in H<sub>2</sub>-air mixtures. A computational fluid dynamics (CFD) model has been developed to determine the MIE by spark for mixtures at ambient temperature with 10%-55% H<sub>2</sub> content in air. Preliminary results have shown good agreement with experiment and the model will be further developed to numerically evaluate the MIE in mixtures at cryogenic temperature.

## 5.2 Electrostatics of cryogenic releases

KIT investigated the electrostatic ignition of cold jets and plumes using the DISCHA experimental setup and the CRYOVESSEL, both described above. In the DISCHA-series two field mills were used while for the CRYOSTAT tests three electric field mills were available. In the DISCHA-experiments the sensors were positioned in the height of the horizontal jet axis with a distance of 0.9 m to it and in distances of 0.5 and 1.5 m to the nozzle. In the CRYOSTAT-experiments the field mills were lined up in a horizontal distance of approx. 2.5 m to the jet axis in the same height as the nozzle (FM1), 50 cm below the jet axis (FM2) and 25 cm below the jet axis (FM3) and with axial distances of -0.2, 1,1 and 2.2 m to the nozzle (FM1 to FM3, respectively), see Figure 9.



Figure 9: Set-up of field measurements in the CRYOSTAT-experiments (left) and snapshot of a cryogenic experiment with LH<sub>2</sub> (right).

In none of the experiments a spontaneous ignition due to the discharge of an electric field was observed. In both facilities no significant field built-up was observed for releases at ambient reservoir temperature. In contrast to this much higher field values were measured in the cryogenic DISCHA-experiments at 80 K, although a considerable scatter in the values was observed, especially when experiments with similar initial conditions were performed on different days with different ambient conditions. Due to the limited data for randomly changing ambient conditions no detailed correlation for changing humidity and temperature values could be derived, but a clear trend towards higher extreme values for larger nozzles and higher initial pressures was observed (left graph of Figure 10). The pressure limitations with the CRYOSTAT-facility might be the reason for the low field values that were measured also for the LH2-releases. So only the data acquired with the DISCHA-facility were used for the formulation of the electric field generation model model:

$$\begin{aligned} \text{Positive Electric Field Built-up / (V/m):} & \quad E(+)\leq(4\cdot dNz + 1)\cdot pini \\ \text{Negative Electric Field Built-up / (V/m):} & \quad E(-)\leq(-14\cdot dNz - 11)\cdot pini \end{aligned}$$

with diameter of nozzle  $dNz$  / mm and initial storage pressure  $pini$  / bar.

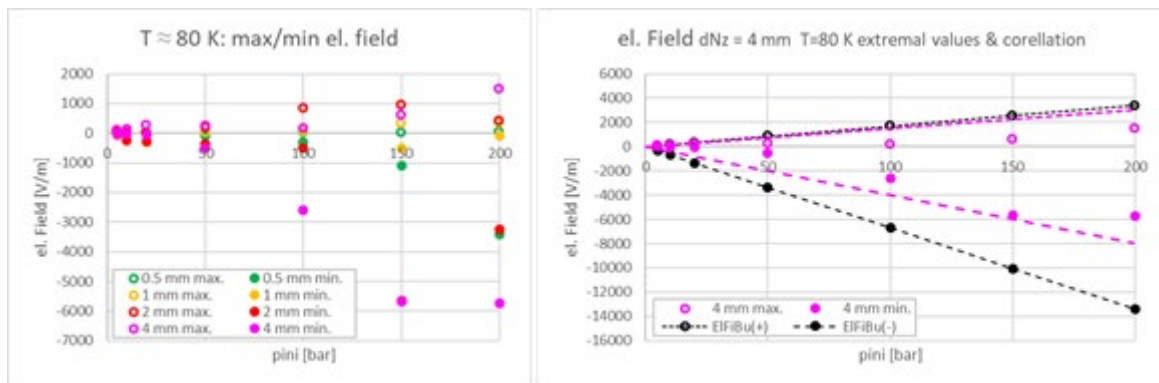


Figure 10: Extremal field values measured in the cryogenic DISCHA-experiments (left) and correlation to estimate these extremal values for the 4-mm-nozzle (right).

A series of experiments were carried out by HSE and were designed to measure two distinct modes of charging; firstly charging due to charge separation near to the LH2/pipe interface, monitored via the wall current from an electrically isolated section of pipework and secondly, charging of the cloud generated by a jet (Figure 11). The latter obviously have a close relation to the electrostatic tests of PS/KIT described above. The experiments measuring wall current were carried out as part of the release experiments described in Section 4, so that measurements were obtained over a wide range of flow conditions. It was observed that the flow of LH2 in pipes did cause electrostatic charges and certain conditions encouraged it. In some cases, the wall current exceeded the measurement range of the instrument. The conditions under which higher wall currents occurred could not be reliably determined, although there are indications that this was associated with two-phase (vapour / liquid) flow within the pipe. From the plume measurements, it was clear that while a transient field can be measured, a hazardously charged plume forming from an established cryogenic jet is unlikely for the initial conditions of these experiments.

The experimental results lead to the assumption that the main reason for electrostatic field built-up is connected with ice crystals that form at cold nozzle prior to release and that are blown off in the initial phase of the release.



Figure 11: Left: Faraday cage for plume measurements. Right: Electrically isolated pipe section.

### 5.3 Ignition above a pool

With the PS/KIT POOL-facility described above also experiments on the ignition of LH<sub>2</sub>-spills were performed. In general the results of the unignited tests performed before served for the planning of the experiments with ignition. The instrumentation above the pool was removed (compare sketch in Figure 6) and replaced by 6 fast pressure sensors. The gas cloud above the pool was ignited using two electrodes in between which a high frequency spark (60 kV, 200 Hz) was generated. In total 14 ignited POOL-experiments with the four substrates concrete, sand, water and gravel were performed. Ignition time and location were varied. The ignition was initiated during the evaporation phase after the second filling of the pool, since after the first filling vigorous boiling behaviour above the still rather warm substrate occurs. After the second filling the boiling behaviour above the precooled substrate is calmer and thus the filling level and concentration measurements give more precise values.

In the experiments different degrees of damage were observed for the different substrate materials. For the substrates with a rather low porosity almost no (water, upper left image in Figure 12) or only minor damage was observed (concrete and sand, center images in upper row of Figure 12), while in the sole experiment with the highly porous substrate of gravel a complete destruction of the facility occurred (Gravel04, upper right image and lower row in Figure 12). The reason for this exceptional behaviour is most likely the higher amount of LH<sub>2</sub> that is also located in the free space in between the stones of the substrate layer, but also air components that condensed or froze at the cold substrate during the LH<sub>2</sub>-evaporation phase in between the two filling procedures.

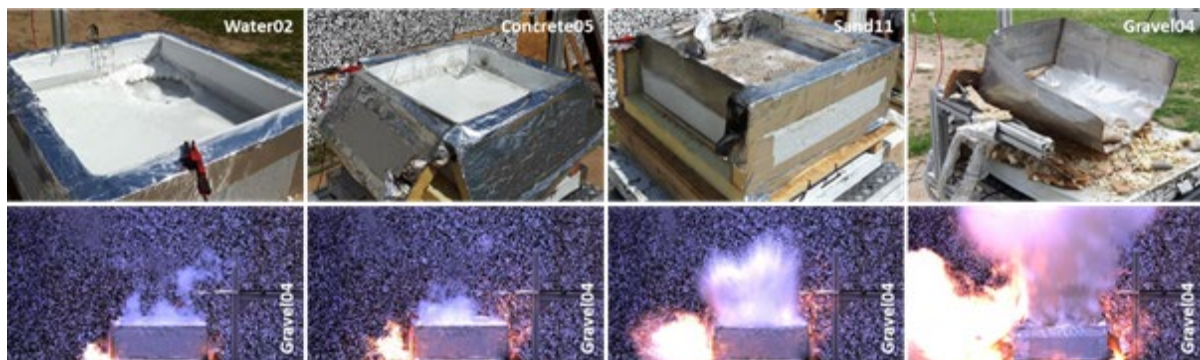


Figure 12: Different degrees of damage to the facility observed in the ignited pool experiments for the different substrates (upper row) and High-Speed video sequence of the final combustion event in experiment Gravel04 (2000 fps, lower row).

## 6.0 RESULTS OF WP 5 - PHENOMENA COMBUSTION

In WP5 experimental and analytical studies on cryogenic hydrogen combustion were performed, addressing laminar/turbulent combustion and detonation in a channel geometry, hydrogen jet ignition and jet fire radiation, burning LH2 pool behaviour, radiation characteristics; cryogenic hydrogen combustion in a layer geometry relevant to flame spread over the spill of LH2.

### 6.1 Combustion experiments

The first series of more than 100 experiments was made with the cryogenic combustion tube CRYOTUBE with L=5 m and 54-mm id and three blockage ratios BR = 0, 30 and 60%. About half of the experiments were made with hydrogen-air mixtures at cryogenic temperatures (approx. 80 to 130 K). The temperature was supported by the location of the tube under a layer of LN2 at T=77K (Figure 13). Subsonic, supersonic deflagrations and detonations were monitored for cryogenic hydrogen combustion by light sensors and pressure gauges located along the tube.

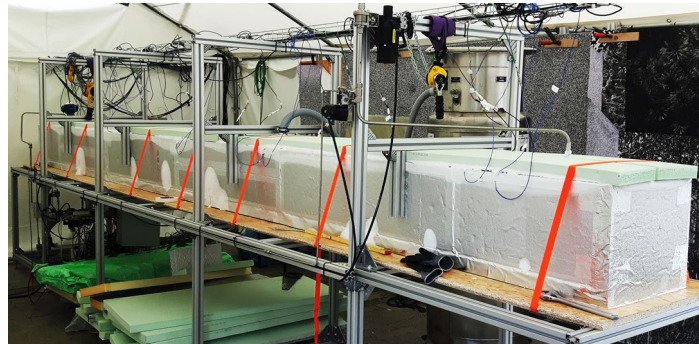


Figure 13: CRYOTUBE immersed in a bath of LN2 with supporting structure.

The critical conditions for flame acceleration to the speed of sound or detonation were evaluated as a function of initial temperature. Particularly at 100 K, it shows a much higher hydrogen concentration of 16% H2 leading to sonic deflagration than that of 9.6% H2 predicted by advanced extrapolation of existing high temperature data before the tests. The correlation based on current experiments is quite simple and useful in a very wide range of initial temperatures  $T = 90 - 650$  K:

$$\sigma^* = 2200 \cdot T^{-1.12}$$

The run-up distance to the speed of sound or detonation in a smooth channel (BR=0) at cryogenic temperatures is two times shorter than at ambient temperature. For the first time, a steady-state flame propagation regime in a smooth channel with the speed of sound in combustion products very often occurs in cases if the detonation is suppressed.

The detonation cell sizes at cryogenic temperature  $T = 100$ K are evaluated on the basis of existing criteria for detonation onset in smooth and obstructed tubes and can be approximated by a polynomial function of hydrogen concentration [H2]:

$$\lambda[\text{mm}] = 0.0006724[\text{H2}]^4 - 0.1039[\text{H2}]^3 + 6.0786[\text{H2}]^2 - 159.74[\text{H2}] + 1603.3$$

It appears that the detonation cell sizes for hydrogen-air mixtures at cryogenic temperature  $T=100$ K only insignificantly differ from that at ambient conditions. After knowing the detonation cell size based

on detonation cell size, all known DDT criteria can be used to assess the detonability of hydrogen –air mixtures in different geometries and scales at cryogenic temperatures.

The maximum combustion pressure at cryogenic temperatures is 2-3 times higher than that for ambient conditions. Theoretically, the maximum combustion pressure for sonic deflagration, which is roughly equal to adiabatic combustion pressure, is proportional to the temperature ratio  $T_0/T$ , where  $T_0 = 293\text{K}$  and  $T$  is the cryogenic temperature. Similarly, the maximum detonation pressure can also be predicted. It demonstrates a very high level of hazard under cryogenic hydrogen combustion. Even a sonic deflagration can be 1.5 times more dangerous than the detonation of the same hydrogen-air mixture at ambient conditions.

Transient cryogenic hydrogen jet fire behaviour, including scaling and radiation properties is investigated with the DISCHA facility (Figure 4). Hydrogen inventory will be changed depending on the initial pressure from 4.4 to 138 g H<sub>2</sub> with initial pressure changes from 0.5 to 20 MPa and LN<sub>2</sub> temperature about 80K. Similar as for the unignited discharge experiments the nozzle size was varied from 1-4 mm id. Measurements consisted of background imaging system (BOS) combined with a high speed camera, fast pressure sensors and thermocouples. Additionally a thermo-vision FLIR camera allowed monitoring the transient temperature fields. With known mass flow rate and hydrogen distribution profile as a function of initial pressure and temperature, hydrogen ignition phenomena and further flame development are investigated with respect to maximum combustion pressure, temperature and heat flux radiation for model validation and hazard distance evaluation.

Unburned cold hydrogen jet was ignited with different delay time after jet initiation at different distances from the nozzle. Then, a strong explosion with formation of a spherical shock wave might occur just after ignition (Figure 14). The over-pressure from 0.04 to 0.115 MPa corresponds to a visible shock wave velocity from 390 to 480 m/s measured by high speed BOS imaging.

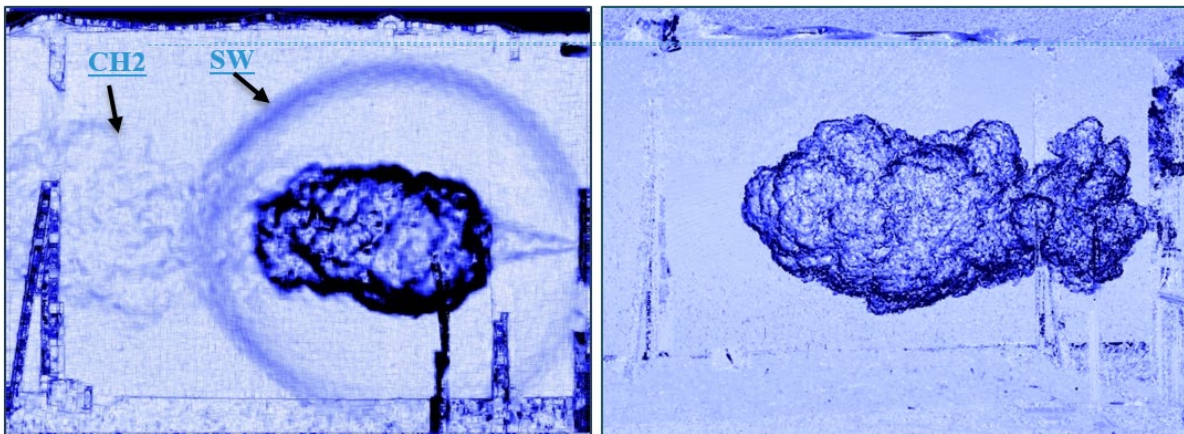


Figure 14: A shock wave formation (left) and a stationary jet fire (right) established under ignition of 4-mm nozzle and 20 MPa pressure hydrogen release: SW –shock wave; CH<sub>2</sub> –unignited hydrogen.

A sequence of frames with temperature distribution is obtained by thermo-vision FLIR-Kamera (15 fps) (Figure 15). For ambient conditions 285K the local maximum combustion temperature changes from 1100 to 540K corresponding to maximum heat flux of 85 kW/m<sup>2</sup>. At the same time, the average integral heat flux of whole surface is about 6.5 kW/m<sup>2</sup>. At cryogenic temperature of 80K, the maximum temperature changes from 1330 to 710K corresponding to maximum heat flux of 177 kW/m<sup>2</sup> in the center of jet fire. The average integral heat flux of whole surface is about 11 kW/m<sup>2</sup>. The reason of such difference is four times larger hydrogen inventory and also 2.5 times higher mass flow rate at

cryogenic temperature leading to 1.3 times higher temperature, 2 times higher heat flux of flame radiation, 1.5 times larger flame length and 1.4 times longer release time.

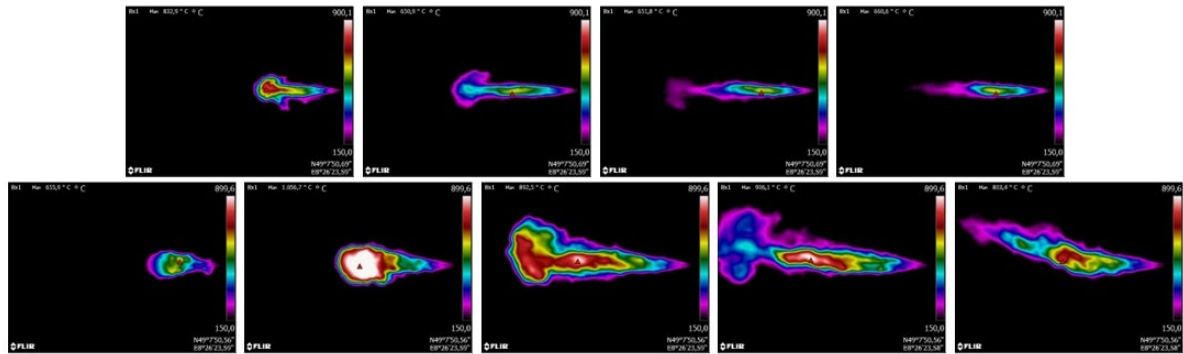


Figure 15: Temperature distribution within jet fire structure. Jet fire radiation for 2-mm nozzle and 10 MPa of initial pressure at  $T=285$  K (upper) and  $T=80$  K.

Using the pressure records and the results of extensive optical observation with up to five cameras the ignition and combustion behaviour of the jets could be analysed.

After ignition flame can either burn back to nozzle or not. This difference is important since in case the flame burns back to the nozzle it will continue burning when ignition source is turned off, while in case the flame does not burn back to the nozzle it will quench after the ignition source is turned off. Using sensor records and optical observation on flame behaviour tests can be divided in two groups, where the flame burns back to the nozzle or not. When this data is combined with the results of the H<sub>2</sub>-concentration measurements of the unignited tests a clear trend can be observed (Figure 16, left).

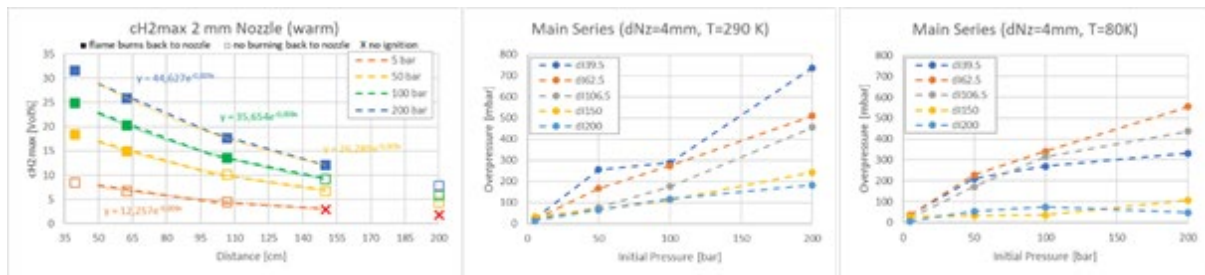


Figure 16. Left: combination of H<sub>2</sub>-concentration measurements (dashed lines) and resulting extrapolation of H<sub>2</sub>-concentrations with combustion behaviour (symbols). Center and right: examples for maximum measured overpressures in experiments at ambient and cryogenic temperature.

For very low H<sub>2</sub>-concentrations in the ignition position no ignition occurs, while for H<sub>2</sub>-concentrations lower than approx. 10 Vol% the jet is ignited but does not burn back to the nozzle. For H<sub>2</sub>-concentrations higher than approx. 10 Vol% in the ignition position the flame burns back to the nozzle. Concerning the combustion overpressures also several trends were observed (Figure 16 center and right). In general, the maximum measured overpressures increase with increasing nozzle diameter, while the gas temperature in the vessel seems to have no significant influence on the maximum pressure load. But at ambient gas temperature the measured overpressures increase with decreasing ignition distance, while in the cryogenic tests the highest overpressures are measured for an ignition distance of 62.5 cm.

## 6.1 Modelling of combustion phenomena and simulations

UWAR conducted large eddy simulation (LES) for selected cases of these unsteady ignited cryogenic hydrogen jets using the rhoReactingFOAM solver within OpenFOAM. The one-equation eddy-viscosity SGS model for compressible flows is used in which a transport equation is solved to resolve the Subgrid Scale (SGS) kinetic energy. The eddy dissipation concept (EDC) model is used for combustion, which is accounted for with detailed hydrogen chemistry. The finite volume discrete ordinates model (FVDOM) is employed to solve the radiative heat transfer equation. For the ignition hot spot located 1.0 m from the nozzle, the instantaneous distributions of the temperature are shown in Figure 17. Spotted flame kernels are formed around the jet tip. The flame kernel then propagates outwards but cannot propagate towards the jet center. It is mainly due to the fact that the low temperature of the hydrogen impedes the chemical reaction on the jet tip. The flame propagates to the sides of the jet and then the flame area expands, as shown by the snapshots from 15 ms to 17 ms.

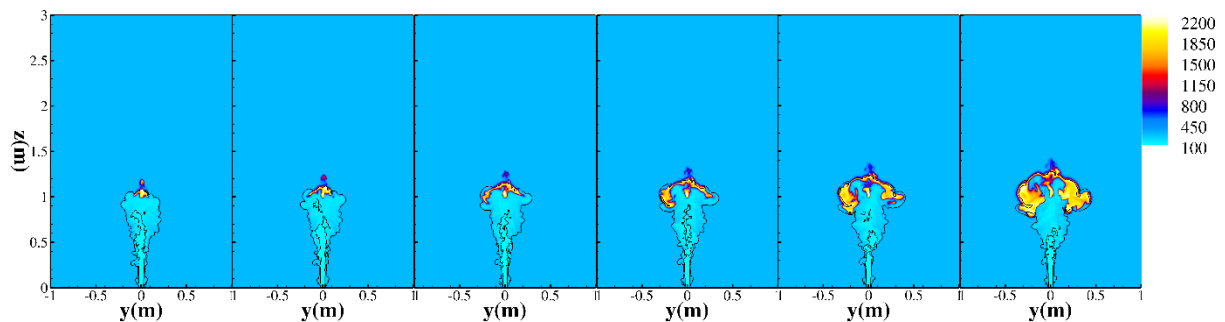


Figure 17: Development of the flame kernel for ignition at 1.0 m with the time from 12 ms to 17 ms. Here the contours are plotted from the predicted temperature (K) and the black iso-lines denote regions with the flammability limit, MolH<sub>2</sub> = (0.040, 0.756).

For ignition at 1.5 m the characteristics the dynamic evolution of the flame changes considerably. The unsteady flame dynamics are determined by the complex interactions among turbulence, fuel-air mixing at cryogenic temperature, and chemical reactions.

Ulster University developed a CFD approach to accurately reproduce thermal radiation from hydrogen jet fires [3][4] as proven by validation against experiments in [1][15]. Simulations showed that buoyancy of combustion products for horizontal jet fires has a positive effect on the reduction of the “no harm” distance by temperature. Thermal radiation leads to longer “no-harm” distances in the direction of the jet compared to the hazard distance defined by temperature. Thermal dose proved to be a useful parameter to define hazard distances for emergency personnel, see [2]. The CFD modelling has been supported by the development of an engineering tool for estimation of thermal hazard from cryogenic jet fires, validated against the same battery of experimental tests.

Additionally an empirical correlation for maximum jet fire radiation at  $x/L_f = 0.6$  as a hyperbolic function against a radial distance from the jet axis ( $r/L_f$ )

$$q_{\max} = 0.74 \left( r/L_f \right)^{-1.59} \text{ kW/m}^2 \text{ —}$$

where  $L_f$  is the visible length of jet fire, was used for defining a damage diagram of human’s skin by jet fire radiation. This is compared to the corresponding CFD calculations of UU in Figure 18.

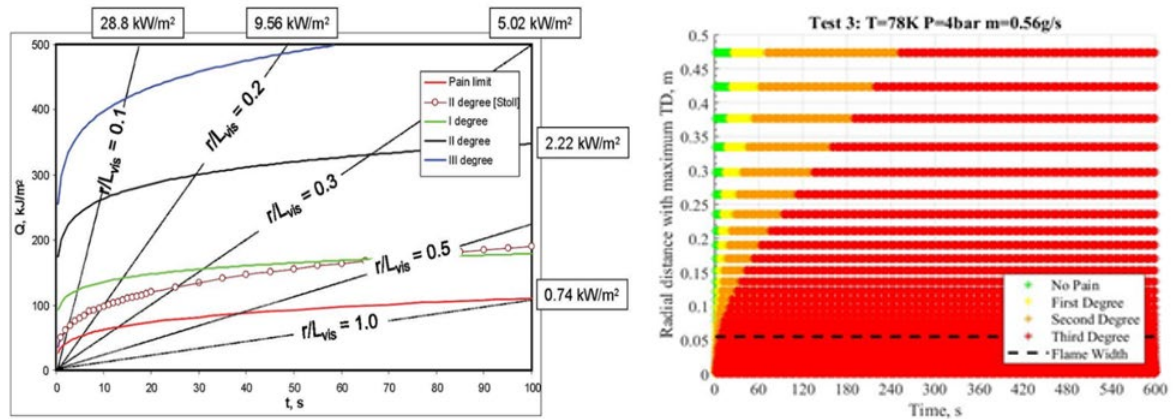


Figure 18: Maximum exposure time for different degree of skin damage by thermal radiation of cryogenic hydrogen jet fire calculated for experimental data KIT (left) and numerical data UU (right).

Additionally, UU performed CFD simulations to assess the effect of cryogenic storage temperature on pressure peaking phenomenon (PPP) from ignited hydrogen releases in a confined space with limited ventilation. Simulations showed that the decrease of storage temperature for a same nozzle diameter and storage pressure causes an increase in hydrogen mass flow rate, and, thus, up to twice higher peak overpressure for a decrease of storage temperature from 277 K to 100 K (storage pressure 11.78 MPa).

## 7.0 IMPLEMENTATION - EXPLOITATION AND DISSEMINATION (WP6)

The outcomes of the pre-normative research are multiple. The new unique experimental data generated within WP3-5 are being made openly available on KIT open research data repositories [14]. Data fulfil Horizon 2020 requirements of being findable, accessible, interoperable and reusable (FAIR).

The generated experimental data were employed to develop and validate analytical models, and to generate empirical and semi-empirical engineering correlations. The engineering correlations and tools aim at quantifying consequences from possible accident scenarios and associated hazard distances, with the goal to support inherently safer design of LH2 systems and recommendations for Regulations, Codes and Standards (RCS). A unified template has been used to describe the engineering correlations and tools, to ease a potential future implementation into existing and/or future integrated platforms for hazards and risks assessment, e.g. the e-Laboratory developed within the ongoing project Net-Tools. The 13 engineering correlations and tools are gathered and described in detail in PRES�HY report D6.5 [5].

The up-to-date knowledge generated during the project has been gathered in the form of a chapter on safety of liquid and cryo-compressed hydrogen [23] providing a review of the state-of-the-art, a description of LH2 relevant phenomena and key experimental results, developed models and engineering correlations, prevention and mitigation techniques, etc.

The guidelines underpin the inherently safer design and operation of LH2 systems and infrastructure, addressing the areas where specific RCS have not been established yet or where they are not suitable for use in public space. The innovative results, strategies and engineering solutions developed during the project have been included in the guidelines. They contained results from the three main topics addressed in PRES�HY: cryogenic hydrogen release and dispersion, ignition and combustion of cryogenic hydrogen-air mixtures. The relevant part of the developed guidelines, including the engineering correlations, have been extracted and expressed in concise language for use by SDOs as

recommendations for RCS. In addition, a roadmap to bring these recommendations to international bodies has been proposed.

The potential benefits of LH2 systems and infrastructure deployment in the FCH sector, particularly with regards to the mobility sector, have been analysed and reported in a White Paper on LH2 [13]. The document motivates the use of LH2 as a safe storage option for hydrogen and as a fuel, by comparing the LH2 hazard profiles to compressed gaseous hydrogen. The White Paper explains the economic benefits of storing and transporting LH2 in large scale or over long distances. The scope of the White Paper is to impact the policy making process and influence the development and spread of FCH technology employing liquid or cryo-compressed hydrogen.

The PRESLHY outcomes have been extensively presented and disseminated at international meetings and events relevant to several aspects of hydrogen safety, such as IEA HIA Task 37 meetings, the Research Priorities Workshop by HySafe, ISO/TC 197 Hydrogen Technologies meeting, the International School Progress in Hydrogen Safety, symposiums, conferences, etc. A flyer of the project was developed in November 2018 and distributed at several dissemination events. The project key results and progresses achieved up to date have been disseminated through 4 newsletters issues. Four workshops have been organised within the consortium and HySafe networks to exchange knowledge and expertise through sessions dedicated to special measurement technologies, experimental or numerical procedures and tools. A workshop on “LH2 Safety - production, transport and handling” was organised as a joint initiative by PRESLHY and SH2IFT projects. The event took place on the 6th March 2019 at Gexcon AS facilities in Bergen, Norway. PRESLHY consortium organised a series of three ad-hoc online workshops focused on the review of experimental outcomes.

PRESLHY dissemination activities culminated with the online project conference on 5-6 May 2021. The conference programme includes 39 presentations from PRESLHY consortium and invited international speakers, providing a throughout overview of the state of the art and worldwide research on safety of liquid hydrogen. The dissemination conference addresses the potential impact of the project outputs on the international community working on hydrogen and fuel cell technologies.

The main impact of the dissemination and exploitation activities consists of the extraction and translation of the project scientific findings into suitable information and tools for international SDOs, regulatory bodies and industry, who represent a large part of the targeted users. To this end, PRESLHY project was presented to the ISO TC 197 committee, establishing a Preliminary Working Item (PWI24077) on “Safe Use of Liquid Hydrogen in Non-industrial Settings” with unanimous support by the committee. The PRESLHY coordinator, was nominated “project manager” of the PWI, and PRESLHY progress has been regularly reported at the ISO committee’s plenary meetings. In late 2020 the PWI was turned into the Task Force 2 of the ISO TC 197 WG29 with the objective to review the ISO TR 15916:2015 and to develop a dedicated chapter on safety of LH2 in this generic standard by 2022. So the updated state-of-the-art and improved understanding will be translated into a normative reference, which shall help introducing LH2 safely for scaling up hydrogen use for the future sustainable energy systems.

## **8.0 ACKNOWLEDGEMENTS**

The PRESLHY acknowledges the support granted by the European Fuel Cell and Hydrogen Joint Undertaking FCH JU under the Project ID 779613.

HSE acknowledges funding from its sponsors Shell, Lloyd's and Equinor.

## 9.0 LITERATURE

- [1] Breitung, W., Stern, G., Vesper, A., Friedrich, A., Kuznetsov, M., Fast, G., Oechsler, B., Kotchourko, N., Travis, J.R., Xiao, J., Schwall, M., “Final Report: Experimental and theoretical investigations of sonic hydrogen discharge and jet flames from small breaks,” 2009
- [2] Cirrone, D., Makarov, D. and Molkov, V., Cryogenic hydrogen jets: flammable envelope size and hazard distances for jet fire, International Conference on Hydrogen Safety, 2019, Adelaide, Australia.
- [3] Cirrone, D., Makarov, D. and Molkov, V., “Thermal radiation from cryogenic hydrogen jet fires,” Int. J. Hydrogen Energy, vol. 44, no. 17, pp. 8874–8885, 2019, doi: 10.1016/j.ijhydene.2018.08.107
- [4] Cirrone, D. Makarov, V. Molkov, “Near Field Thermal Dose of Cryogenic Hydrogen Jet Fires,” in proceedings of the Ninth International Seminar on Fire and Explosion Hazards (ISFEH9), 2019, pp. 1360–1366
- [5] Cirrone, D., Makarov, D., Molkov, V., Venetsanos, A., Coldrick, S., Atkinson, G., Proust, C., Friedrich, A., Kuznetsov, M., PRESLHY D6.5 Detailed description of novel engineering correlations and tools for LH2 safety, version 2, 2021.
- [6] Cirrone, D., Makarov, D., Kuznetsov, M., Friedrich, A. and Molkov, V. (2021), Effect of heat transfer through the release pipe on simulations of cryogenic hydrogen jet fires and hazard distances, International Conference on Hydrogen Safety 2021.
- [7] Giannissi, S.G., Venetsanos, A.G., Cirrone, D., Molkov, V., Ren, Z., Wen, J., Friedrich, A., Vesper, A., "Cold hydrogen blowdown release: an inter-comparison study", 9th Int. Conf. on Hydrogen Safety, 21-23 Sept. 2021, Edinburgh, UK.
- [8] Giannissi, S.G., A.G. Venetsanos, Vyazmina, E., Jallais, S., Coldrick, S., Lyons, K., CFD simulations of large scale LH2 dispersion in open environment, 9th Int. Conf. on Hydrogen Safety, 21-23 Sept. 2021, Edinburgh, UK.
- [9] Hecht, E. S. and Panda, P. P., “Mixing and warming of cryogenic hydrogen releases,” Int. J. Hydrogen Energy, vol. 44, pp. 8960–8970, 2019.
- [10] Jallais, S. and Bernard, L., State of the art analysis, PRESLHY Project Deliverable Number: 13 (D2.2), 2018; [https://hysafe.info/wp-content/uploads/sites/3/2020/01/PRESLHY\\_D2.2\\_State-of-the-art-analysis\\_20191119\\_V1p1.pdf](https://hysafe.info/wp-content/uploads/sites/3/2020/01/PRESLHY_D2.2_State-of-the-art-analysis_20191119_V1p1.pdf)
- [11] Jallais, S. and Bernard, L., LH2 Installation Description, PRESLHY Project Deliverable Number: 14 (D2.3), 2018, [https://hysafe.info/wp-content/uploads/sites/3/2020/01/PRESLHY-D2.3-LH2-Installation-description\\_20191119\\_V1p1.pdf](https://hysafe.info/wp-content/uploads/sites/3/2020/01/PRESLHY-D2.3-LH2-Installation-description_20191119_V1p1.pdf)
- [12] Jallais, S., Phenomena Identification and Ranking Table (PIRT) Analysis, PRESLHY Project Deliverable Number: 16 (D2.5), 2018, [https://hysafe.info/wp-content/uploads/sites/3/2020/01/PRESLHY-D2.5-PIRT\\_20191119\\_V1p1.pdf](https://hysafe.info/wp-content/uploads/sites/3/2020/01/PRESLHY-D2.5-PIRT_20191119_V1p1.pdf)
- [13] Jordan, T., PRESLHY White Paper, PRESLHY Project Deliverable D6.4 2021,
- [14] KIT Open Repository [bibliothek.kit.edu/English/kitopen.php](http://bibliothek.kit.edu/English/kitopen.php) (last access on 17 May 2021)
- [15] Panda, P.P. and Hecht, E. S., “Ignition and flame characteristics of cryogenic hydrogen releases,” Int. J. Hydrogen Energy, vol. 42, no. 1, pp. 775–785, 2017, doi: 10.1016/j.ijhydene.2016.08.051.
- [16] Tchouvelev, A.V., Regulations, Codes and Standards (RCS) Analysis; Project Deliverable Deliverable Number: 12 (D2.1), 16 May 2018; [https://hysafe.info/wp-content/uploads/sites/3/2020/01/HySafe\\_RCS-Report\\_D2.1\\_V1p1\\_20200109.pdf](https://hysafe.info/wp-content/uploads/sites/3/2020/01/HySafe_RCS-Report_D2.1_V1p1_20200109.pdf)
- [17] Ustolin F., Tolias I., Giannissi S., Venetsanos A., Paltrinieri N., A CFD analysis of liquefied gas vessel explosions using the ADREA-HF code, 9th Int. Conf. on Hydrogen Safety, 21-23 Sept. 2021, Edinburgh, UK.

- [18] Venetsanos A.G., Homogeneous non-equilibrium two-phase choked flow modelling, *Int. J. of Hydrogen Energy*, 43, 2018, 22715-22726
- [19] Venetsanos A.G., Giannissi S., Proust C., CFD validation against large scale liquefied helium release, 8th Int. Conf. on Hydrogen Safety, 24-26 Sept. 2019, Adelaide, Australia.
- [20] Venetsanos A.G., Choked two-phase flow with account of discharge line effects, 8th Int. Conf. on Hydrogen Safety, 24-26 Sept. 2019, Adelaide, Australia.
- [21] Venetsanos A.G., Giannissi S., Toliás I., Friedrich A., Kuznetsov M., Discharge modelling of cryogenic hydrogen including discharge line effects, 9th Int. Conf. on Hydrogen Safety, 21-23 Sept. 2021, Edinburgh, UK.
- [22] Venetsanos A.G., Ustolin F., Toliás I., Giannissi S., Momferatos G., Coldrick S., Atkinson G., Lyons K., Jallais S., Discharge modelling of large scale LH2 experiments with an engineering tool, 9th Int. Conf. on Hydrogen Safety, 21-23 Sept. 2021, Edinburgh, UK.
- [23] Verfondern, K., Cirrone, D., Makarov, D., Molkov, V., Coldrick, S., Ren, Z., Wen, J., Proust, C., Friedrich, A., Jordan, T., PRESLHY D6.1 Handbook of hydrogen safety: Chapter on LH2 safety, 2021.